coatings

MDPI

Article

Water Pipes Corrosion Inhibitors for Q235 Steel in Hydrochloric Acid Medium Using Spiropyrazoles Derivatives

A. M. Eldesoky [1,2,*], Hala. M. Hassan [3,4], Abdu Subaihi [2], Abeer El Shahawy [5,*] and Thoraya A. Farghaly [6,7]

1 Engineering Chemistry Department, High Institute of Engineering &Technology (New Damietta), New Damietta 34517, Egypt
2 Al-Qunfudah Center for Scientific Research (QCSR), Chemistry Department, Al-Qunfudah University College, Umm Al-Qura University, Al Qunfudhah 21912, Saudi Arabia; aasubaihi@uqu.edu.sa
3 Textile Technology Department, Industrial Education College, Beni-Suef University, Beni Suef 62511, Egypt; dr.halamahfooz@yahoo.com
4 Chemistry Department, Faculty of Science, Jazan University, Jizan 45142, Saudi Arabia
5 Department of Civil Engineering, Faculty of Engineering, Suez Canal University, Ismailia 41522, Egypt
6 Department of Chemistry, Faculty of Science, University of Cairo, Giza 12613, Egypt; thoraya-f@hotmail.com or tamohamed@uqu.edu.sa
7 Department of Chemistry, Faculty of Applied Science, Umm Al-Qura University, Makkah Almukkarramah 21955, Saudi Arabia
* Correspondence: a.m.eldesoky79@hotmail.com (A.M.E.); abeer_shahawi@eng.suez.edu.eg (A.E.S.)

Received: 18 December 2019; Accepted: 1 February 2020; Published: 12 February 2020

Abstract: Water pipes and drinking water quality deterioration in distribution systems and sea water desalination impose the use of corrosion inhibitors. The protective effect of spiropyrazole derivatives against Q235 steel and its adsorption performance were examined in solution of 1 M HCl utilizing TP (Tafel polarization), electrochemical frequency modulation (EFM), and electrochemical impedance spectroscopy (EIS) tests. The outcome data from hindrance efficiency rise with the dose of inhibitor. The orders of %IE of spiropyrazole derivatives are given: (1) > (2) > (3).It was noted that the values of E_{HOMO} and E_{LUMO} dropping in order run parallel to the improvement in %IE, which support the preceding order. EIS spectra exhibited one capacitive loop and approve the protective ability. Molecular docking was utilized to get a full picture on the binding mode among spiropyrazoles derivatives and the receptor of 3tt8-hormone of crystal structure examination of Cu human insulin derivative. The morphology of protected Q235 steel was evaluated by checking electron magnifying instrument innovation with energy dispersive X-beam spectroscopy (SEM–EDX).

Keywords: spiropyrazoles; 3tt8-hormone; Q235 steel; SEM–EDX; molecular docking

1. Introduction

Corrosion in distribution systems pipes resulted in not only pipe material destruction, but also deterioration in drinking water quality, i.e., water infection with other wastewater or any other water. Which leads to corrosion of valves or pumps in addition to blockage in pipes as a result of solid corrosion products.Unwanted chemical and biochemical reactions that occur in the distribution systems that release iron into distributed water can accumulate, creating tubers [1]. Corrosion measurements (tubers) consist of reactive types that modify the physical and chemical parameters of water in the distribution system not only by releasing Fe oxyhydroxides, but also by interactions, for example, with by-products of chlorinated disinfection [2], nitrates, or with natural organic substance [3]. Salinity

(chloride) is one of the most aggressive substances in seawater. Oxygen in seawater also affects metal pipes corrosion rate. Moreover, the amount of oxygen affected with the temperature, and consequently influences the rate of corrosion [4].

Salts in the sea water cause corrosion inside the surfaces of pipes that transport saltwater in desalination water treatment plants. Also, the existence of air, salts on the ground, moisture, and other factors lead to outside pipe corrosion in the form of small holes or rough surface.

In any case, corrosion causes a short lifetime of the pipe, hydraulic effects, aesthetic effects, including increasing pumping costs, water leaks, and the buildup of corrosion products. Pipe replacement is not possible due to the high cost, so it is necessary to isolate pipe material from water and any corrosive agents [5].

Corrosion inhibitors are largely utilized as a part of industry, as for instance, corrosive pickling of steel and iron, overflow cleaning and preparing, generation of metal and well oil fermentation [6–8]. Improving the acidic environment needed the progress of altered corrosion control tests among which the implementation of chemical restraints has been the most economical test for the hindrance corrosion of acid [9–14]. Several organic composites, such as heterocyclic assembled, acetylenic alcohol, and quaternary ammonium salts are normally utilized as inhibitors in altered industries. The selected atoms adsorbed on the surface of metal among hetero atoms which include N, S, and O due to its protection for the active centers and to form a physical barrier to lowering the transmit of erosion sample to the metal surface [15–21]. The heterocyclic affluences containing nitrogen atoms, like 4-aminoantipyrine (pyrazole derivative) are excellent corrosion hindrance with corrosive solution because rise hindrance of corrosion and prevent the odor irritating for alloys in altered aggressive environment [22–27]. Therefore, the development of novel adjuster inhibitors consisting of a pyrazol ring and the study of the relations among the inhibitors chemical structure and their inhibition led to the greater significance in theoretical points and industrial application.

In this study, the hindrance effect and electrochemical habit of spiropyrazole products for Q235 steel including 1.0 M HCl are given by the TP, EIS) and EFM tests. A few quantum-chemistry tests and molecular docking have been conducted in order to record the inhibition protection to the molecular properties of the altered kind of assembled [28,29].

2. Experimental

2.1. Measurements

This research mimics the actual docking process in which measuring interaction energies of the ligand–protein pair-wise through Docking Server [30]. Docking computations were carried out on a spiropyrazoles protein model. Kollman united atom kind charges, Essential hydrogen atoms, and solvation parameters were additional with the support of AutoDock tools [31]. Affinity (grid) maps of 20 × 20 × 20 Å grid points and 0.375 Å spacing were generated utilizing the program Autogrid [32].

2.2. Material and Medium

Q235 steel was utilized for the measurements of corrosion. Its % conformation is 0.16 C, 0.30 Si, 0.53 Mn, 0.055 S, 0.045 P, the rest iron. The corrosion dose (HCl 1.0 M) (37% analytical grade). The structure of spiropyrazole derivatives utilized for this paper are given in Table 1 [33].

Table 1. Molecular formulas and structure of spiropyrazoles products.

Cpd. No.	Name	Structure	Molecular Weight &Chemical Formula
(1)	2′,3′,6,7,8,9-Hexahydro-2′-phenyl-5′-styryl-3′-(3,4,5-trimethoxy-phenyl) spiro[benzocyclo–heptane-6(5H), 4′(4H-pyrazol)-5-one	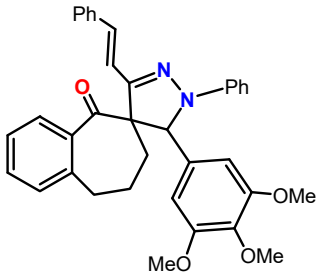	$C_{36}H_{34}N_2O_4$ (558.25)
(2)	3′-(3,4-Dimethoxyphenyl)-2′,3′,6,7,8,9–hexahydro-2′-phenyl-5′-styrylspiro [benzocyclo– heptane–6(5H), 4′(4H-pyrazol)-5-one	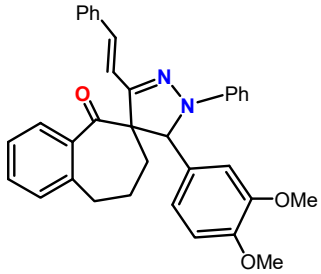	$C_{35}H_{32}N_2O_3$ (528.24)
(3)	3′-(4-Chlorophenyl)-2′,3′,6,7,8,9-hexahydro-2′-phenyl-5′-styryl-spiro [benzocycloheptene-6(5H), 4′(4H-pyrazol)-5-one	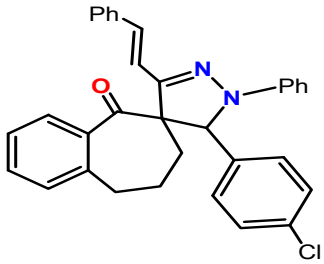	$C_{33}H_{27}ClN_2O$ (502.18)

2.3. Methods

2.3.1. Electrochemical Tests

Electrochemical tests were performed utilizing three thermostat electrodes cell for the electrode cell using a Gamrypotentiostat/galvanostat/ZRA (model PCI300/4). A saturated platinum and calomel electrode were utilized as auxiliary and reference electrodes. All tests were done at the temperature of 25 ± 1 °C. The measurements of potentiodynamic bends were from −50 to 50 V at a rate scan 1 mV S^{-1} after the steady state is approximated (30 min) and the OCP was detected after the electrode was putted for 15 min in the solution test.

The two tests, EFM and EIS were carried out as before with the system of a Gamry framework rely on ESA400. Echem Analyst 5.5 Software was utilized for graphing, drawing, and fitting value. EIS tests were done in a range of frequency of 100 kHz to 10 mHz with amplitude of 5 mV signal-to-signal ac peaks utilized at respective for corrosion potential. EFM had used 2 frequencies 2 and 5 Hz. The frequency base was 1 Hz.

2.3.2. SEM-EDX Tests

The surface of Q235 steel was gotten by observance the coins for 3 days dipping in 1 M HCl existence and lack of seamless dose of spiropyrazoles derivatives. Then, after this time dipping, the coins were lotion gently with water distilled. The surface of alloy was tested utilized an X-ray diffractometer Philips (pw-1390) with Cu-tube (CuKα, l = 1.54051 Å), (SEM, JOEL, JSM-T20, Tokyo, Japan).

2.3.3. Theoretical Study

Accelrys (Material Studio Version 4.4) software for quantum chemical measurements has been utilized.

3. Results and Discussion

3.1. TP Tests

TP tests were conducted to obtain information regarding the kinetics of the anodic and cathodic reactions. Figure 1 demonstrations the TP performance of Q235 steel electrode in corrosive solution nonexistence and attendance unlike dose of spiropyrazoles derivatives (1). Figure 1 shows that the $\%IE_p$ rise as the spiropyrazoles dose rise, while the cathodic reaction is efficient protective, i.e., the adding of spiropyrazoles decrease the anodic liquefaction of alloyand also hindrance the cathodic reactions. Therefore, spiropyrazoles are acts as mixed kind inhibitors.

The (θ) and %IE were measured from relation (1):

$$\%IE_p = \theta \times 100 = [1 - (i^0{}_{corr}/i_{corr})] \times 100 \quad (1)$$

where $i^0{}_{corr}$ and i_{corr} are the current lack and attendance of solution inhibitor, consecutively.

It is evident from Table 2 that the adsorbed inhibitors lessened the surface area for corrosion without effect on the mechanism of alloy corrosion in acidic solution [34,35]. The orders of IE% were: (1) > (2) > (3).

Table 2. Impact of spiropyrazoles derivatives for Q235 steel in in corrosive environments attendance and lack of unlike dose of spiropyrazoles.

Cpd. No.	Conc., M.	$-E_{corr}$ (mV vs. SCE)	$i_{corr} \times 10^{-5}$ (μA cm^{-2})	$\beta_a \times 10^{-3}$ (mV dec^{-1})	$\beta_c \times 10^{-3}$ (mV dec^{-1})	θ	%IE
–	Blank	489	5.02	106	145	–	–
(1)	1×10^{-6}	459	1.3	60	132	0.741	74.1
	3×10^{-6}	469	1.28	91	198	0.745	74.5
	5×10^{-6}	493	1.26	99	152	0.749	74.9
	7×10^{-6}	479	1.24	77	119	0.753	75.3
	9×10^{-6}	488	1.19	79	159	0.7629	76.29
	11×10^{-6}	467	1.05	104	146	0.7908	79.08
(2)	1×10^{-6}	457	1.51	34	56	0.6992	69.92
	3×10^{-6}	491	1.48	87	123	0.7052	70.52
	5×10^{-6}	466	1.45	53	135	0.7112	71.12
	7×10^{-6}	487	1.37	83	121	0.7271	72.71
	9×10^{-6}	458	1.35	62	115	0.7311	73.11
	11×10^{-6}	489	1.25	107	156	0.751	75.1
(3)	1×10^{-6}	439	2.4	52	127	0.5219	52.19
	3×10^{-6}	481	2.05	79	143	0.5916	59.16
	5×10^{-6}	483	1.92	84	129	0.6175	61.75
	7×10^{-6}	462	1.73	67	143	0.6554	65.54
	9×10^{-6}	461	1.64	58	117	0.6733	67.33
	11×10^{-6}	480	1.48	69	123	0.7052	70.52

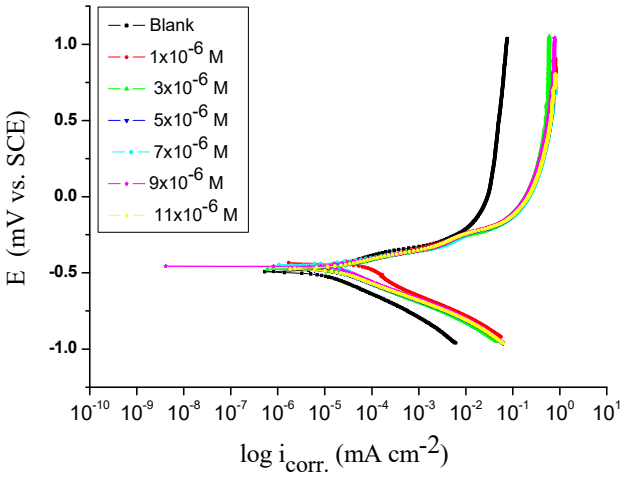

Figure 1. TP diagrams for the corrosion of Q235 steel in corrosive environments in the presence and lack of unlike dose of spiropyrazoles (1) at 25 ± 0.1 °C.

3.2. EIS Tests

One of the most effective tests in corrosion study is EIS. The properties of mechanical materials for surface and electrode motility can be obtained using impedance diagrams [36–40]. Figure 2 illustrated Nyquist (a) and Bode (b) bends given at OCP both in lack and attendance of improving dose of spiropyrazole derivatives. The values from EIS tests for a Q235 steel electrode were given utilizing the equivalent circuit demonstrated in Figure 3.The improvement in the size of the capacitive loop with the attachment of spiropyrazole derivatives demonstrate that a barrier gradually forms on the surface of metal [41,42]. The higher in the size of capacitive loop Figure 2 aimproves, at a fixed inhibitor dose, conformed the order: (1) > (2) > (3). The C_{dl} is measured from Equation (2):

$$C_{dl} = Y_o\ \omega^{n-1}/\sin[n(\pi/2)] \quad (2)$$

where $\omega = 2\pi f_{max}$, f_{max} = the maximum frequency.

After EIS exam the figure of the Nyquist bends, the corrosion procedure was measured principally charged-transfer [43–46]. From Table 3 for the EIS data, we distinguished that the results of Rct improve with increasing the dose of spiropyrazoles and this result in improving in %IE. Data of Cdl are also minor to the maximum spiropyrazole inhibitor range [47,48]. The main merits of EIS are to monitor the corrosion performance of the metal with constant time. The %IEEIS was gotten from the EIS data from Equation (3) [49]:

$$\%IE_{EIS} = [1 - (R^{\circ}{}_{ct}/R_{ct})] \times 100 \quad (3)$$

where $R^{o}{}_{ct}$ and R_{ct} are the resistance values existence and lack of spiropyrazole, consecutively.

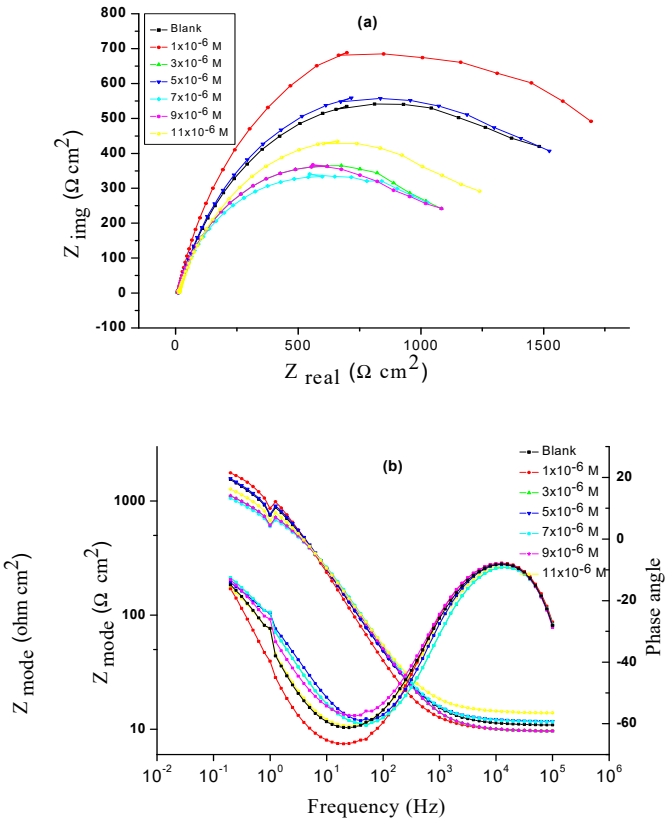

Figure 2. EIS Nyquist (**a**) and Bode diagrams (**b**) for the corrosion of Q235 steel inattendance and lack of unlike dose of compound (1) at 25 ± 0.1 °C.

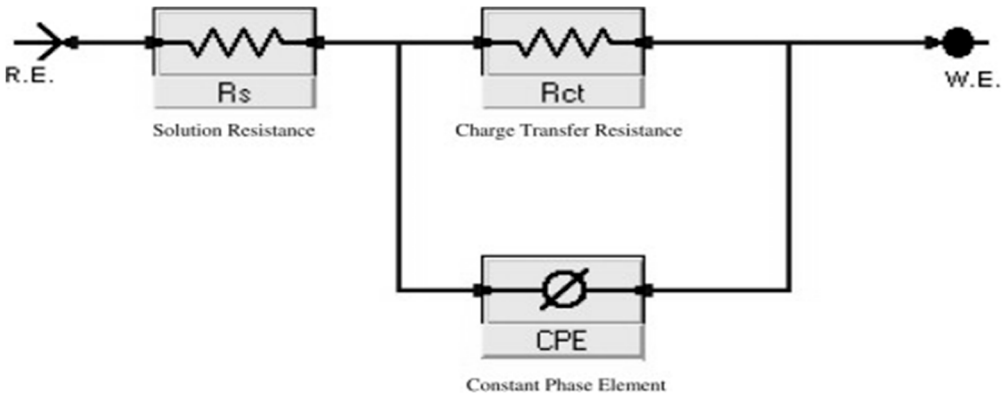

Figure 3. Equivalent circuit utilized to fit EIS data.

Table 3. Parameters given by EIS test for Q235 steel in corrosive environments attendance and lack of unlike dose of spiropyrazoles derivatives.

Cpd. No.	Conc., M.	$R_S \times 10^{-3}$ (Ω cm^2)	$Y_o \times 10^{-6}$	$n \times 10^{-3}$	$R_{ct} \times 10^{-3}$ (Ω cm^2)	$C_{dl} \times 10^{-5}$ (μFcm^{-2})	θ	IE
–	Blank	11.1	18.2	1.01	36.9	8.93	–	–
(1)	1×10^{-6}	9.7	12.6	1.03	178	1.24	0.793	79.3
	3×10^{-6}	9.7	12.2	1.04	179	1.23	0.794	79.4
	5×10^{-6}	10.8	12.7	1.12	194.7	1.22	0.81	81
	7×10^{-6}	10.6	16.8	1.05	220.1	1.29	0.832	83.2
	9×10^{-6}	9.6	16.3	1.07	361.7	1.2	0.898	89.8
	11×10^{-6}	9.7	12.3	1.06	428.1	1.19	0.914	91.4
(2)	1×10^{-6}	9.6	9	1.05	78.61	1.67	0.531	53.1
	3×10^{-6}	11.4	18.3	1.03	105.3	1.31	0.65	65
	5×10^{-6}	13.9	13	1.05	112.3	1.3	0.671	67.1
	7×10^{-6}	15.9	19.8	1.12	119.5	1.29	0.691	69.1
	9×10^{-6}	9.7	12.6	1.04	123.2	1.26	0.7	70
	11×10^{-6}	11.1	19	1.06	134.2	1.25	0.725	72.5
(3)	1×10^{-6}	10	27.6	1.01	42.13	6.24	0.124	12.4
	3×10^{-6}	9.5	13.7	1.02	49.85	2.75	0.26	26
	5×10^{-6}	11.89	18.15	1.05	55.28	1.98	0.332	33.2
	7×10^{-6}	13.37	11.98	1.03	66.76	1.9	0.447	44.7
	9×10^{-6}	9.5	12.99	1.02	67.12	1.83	0.45	45
	11×10^{-6}	13.81	12.98	1.06	77.56	1.7	0.524	52.4

3.3. The Method of EFM

The advantages of EFM test gotten it a perfect for online monitoring of corrosion [50]. The data of EFM in corrosive environments existance and lack of unlike dose of spiropyrazoles was obtain in Figure 4. The results of EFM-tests were applied two unlike models: diffusion complete control of the cathodic reaction was quantified by and the "activation" model [51]. The (i_{corr}), (CF-2 and CF-3), and (βc and βa) were quantified by the higher peaks. The preferable data of CF-2 and CF-3 in Table 4 are parallel to their theoretical numbers of 2.0 and 3.0, individually result in excellent quality of the measured data.

The $\%IE_{EFM}$ raising by improvement the inhibitor dose and was calculated from Equation (4):

$$\%IE_{EFM} = [1 - (i_{corr} i^{o}{}_{corr})] \times 100 \quad (4)$$

where $i^{o}{}_{corr}$ and i_{corr} are current attendance and lack of spiropyrazoles, consecutively.

The order of $\%IE_{EFM}$: (1) > (2) > (3).

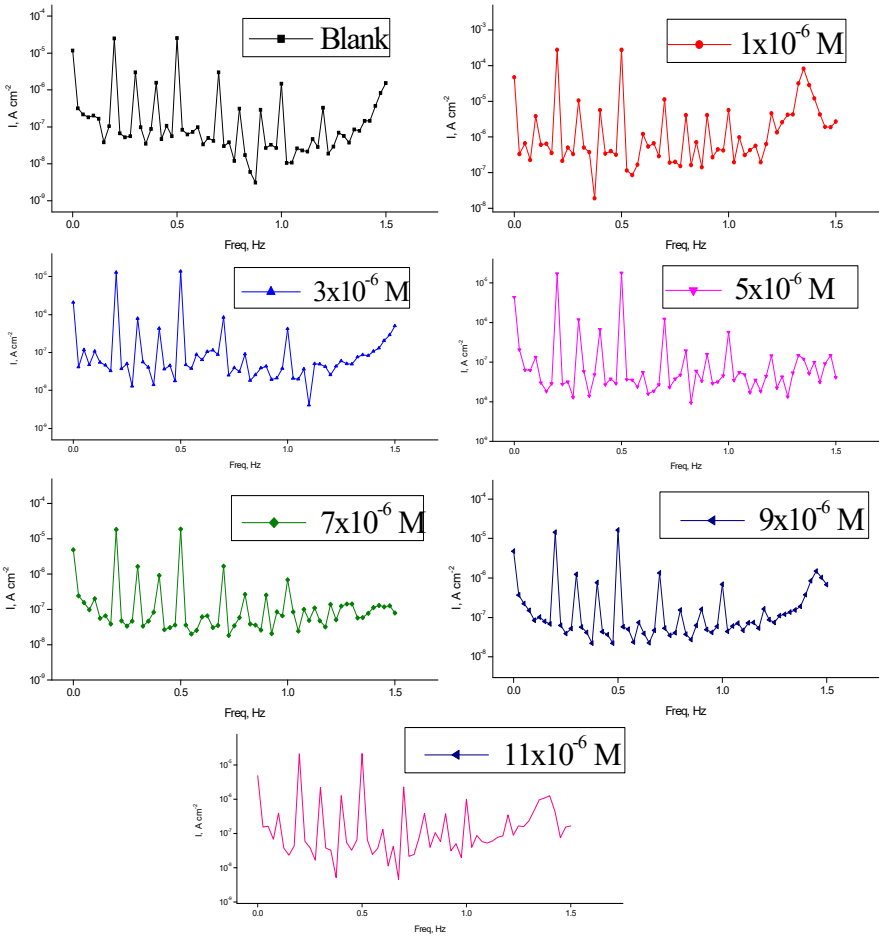

Figure 4. EFM bends for the corrosion of Q235 steel in corrosive environments attendance and lack of unlike dose of spiropyrazoles (1).

Table 4. EFM parameters for Q235 steel in corrosive environments attendance and lack of unlike dose of spiropyrazoles derivatives at 25 ± 1 °C.

Cpd. No.	Conc., M.	i_{corr} (μA cm^{-2})	$\beta_a \times 10^{-3}$ (mV dec^{-1})	$\beta_c \times 10^{-3}$ (mV dec^{-1})	CF-2	CF-3	θ	%IE
–	Blank	58.04	98	331	2.02	2.87	–	–
(1)	1×10^{-6}	21.99	88	350	1.94	2.95	0.6211	62.11
	3×10^{-6}	19.09	82	129	1.89	2.9	0.6711	67.11
	5×10^{-6}	15.29	87	146	1.85	3.02	0.7366	73.66
	7×10^{-6}	14.91	74	105	1.87	3.12	0.7431	74.31
	9×10^{-6}	11.48	46	49	1.89	3.01	0.8022	80.22
	11×10^{-6}	9.33	55	71	2.01	2.74	0.8392	83.92
(2)	1×10^{-6}	32.5	97	193	1.99	2.89	0.44	44
	3×10^{-6}	31.02	121	227	2.02	2.87	0.4655	46.55
	5×10^{-6}	28.8	79	90	2.02	2.91	0.5038	50.38
	7×10^{-6}	28.03	91	195	1.97	3	0.5171	51.71
	9×10^{-6}	27.04	92	165	1.87	2.91	0.5341	53.41
	11×10^{-6}	25.36	84	162	1.93	3.05	0.5631	56.31
(3)	1×10^{-6}	38.22	86	108	1.97	3.08	0.3415	34.15
	3×10^{-6}	37.55	141	298	1.92	2.87	0.353	35.3
	5×10^{-6}	36.32	106	190	1.89	3.14	0.3742	37.42
	7×10^{-6}	35.12	93	189	2.08	3.04	0.3949	39.49
	9×10^{-6}	33.04	105	227	1.83	3.02	0.4307	43.07
	11×10^{-6}	30.34	76	148	1.76	2.78	0.4773	47.73

3.4. Molecular Docking

The docking study presented a favorable contact among spiropyrazoles derivatives and the receptor of 3tt8-hormone of crystal structure analysis of Cu human insulin derivative. The energy calculated is recorded in Table 5 and Figure 5. According to the outcome data in this study, HB diagrams specified that the spiropyrazoles derivatives bind to the proteins via hydrogen bond and disintegrated interactions energies in kcal/mol existed among the spiropyrazoles derivatives with 3tt8 receptor as exposed in Figure 6. Also, based on this value, it can propose that interaction among the 3tt8 receptor and the spiropyrazoles is possible [52]. Further, 2D plot bends of docking with spiropyrazole products are displayed in Figure 7.

Table 5. Energy data gotten in docking measurements of spiropyrazoles derivatives with 3tt8 receptor.

Cpd. No.	Est. Free Energy of Binding (kcal/mol)	Est. Inhibition Constant (K_i) (μM)	vdW+ bond+ Desolve Energy (kcal/mol)	Electrostatic Energy (kcal/mol)	Total Intercooled Energy (kcal/mol)	Interact Surface
(1)	−5.06	193.78	−6.45	−0.03	−6.48	640.460
(2)	−4.92	247.10	−6.57	+0.01	−6.56	594.819
(3)	−6.36	21.62	−7.32	−0.01	−7.33	611.749

Cpd. No.	(A)	(B)
(1)	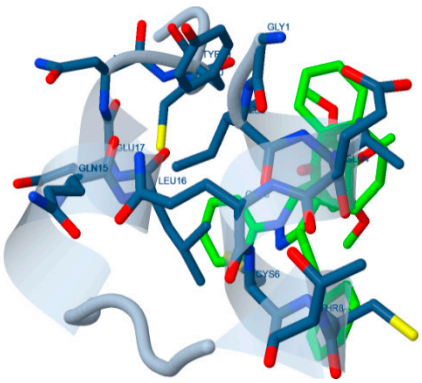	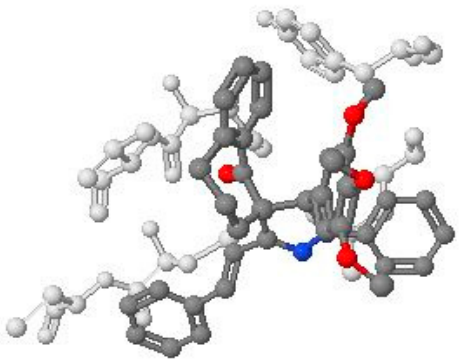
(2)	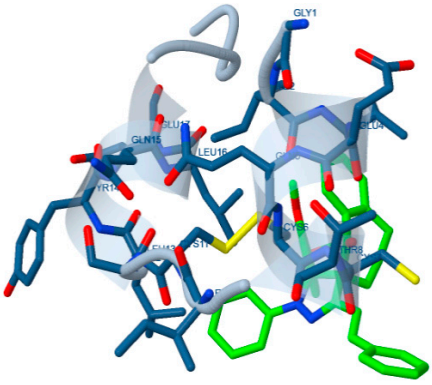	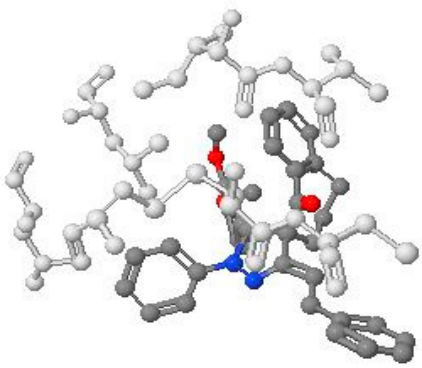

Figure 5. *Cont.*

(3)

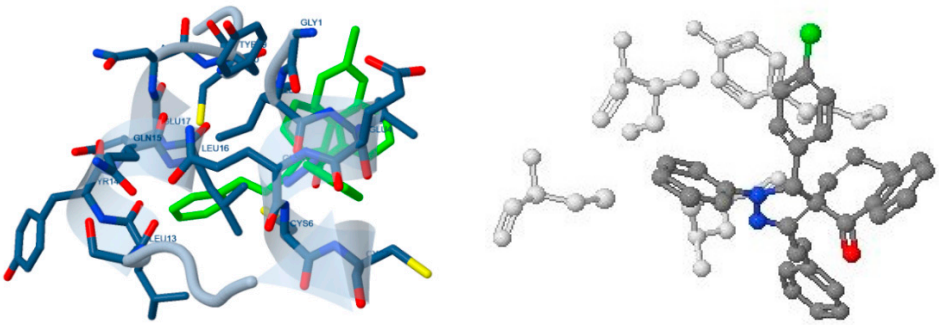

Figure 5. Spiropyrazoles derivatives (green in (**A**) and gray in (**B**)) in interaction with 3tt8 receptor. (For interpretation of the references to color in this figure legend, the reader is referred to the web version of this article).

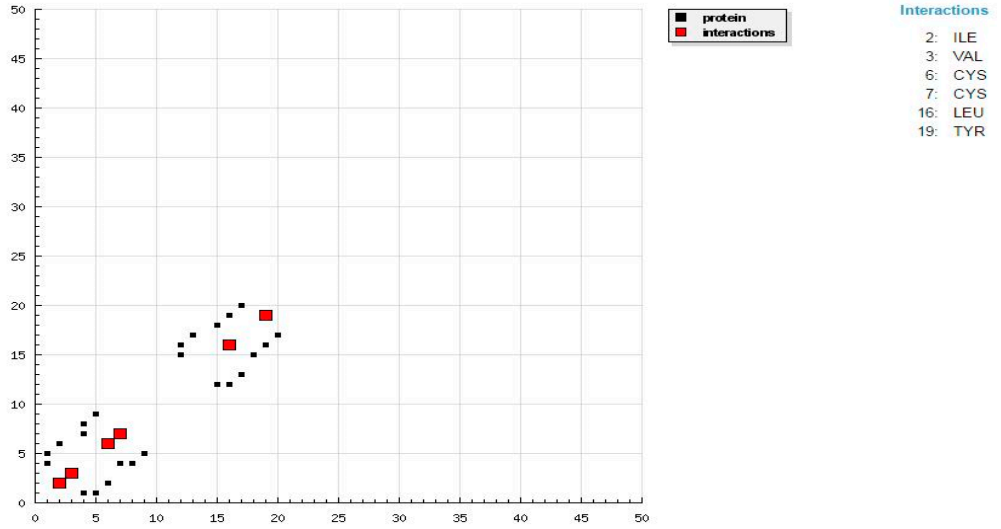

Compound (1)

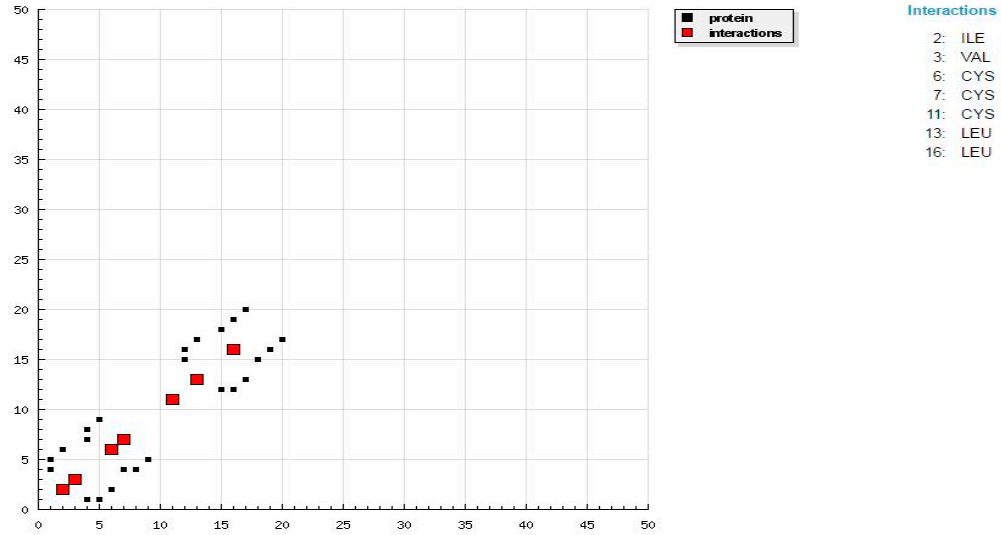

Compound (2)

Figure 6. *Cont.*

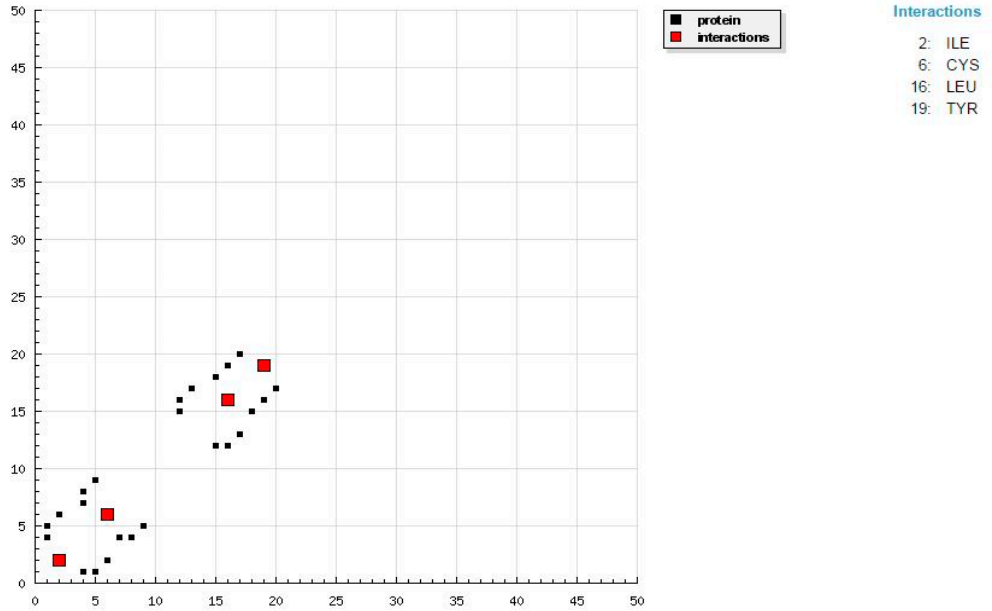

Compound (3)

Figure 6. HB plot of interaction between spiropyrazoles products with receptor of breast cancer mutant 3tt8.

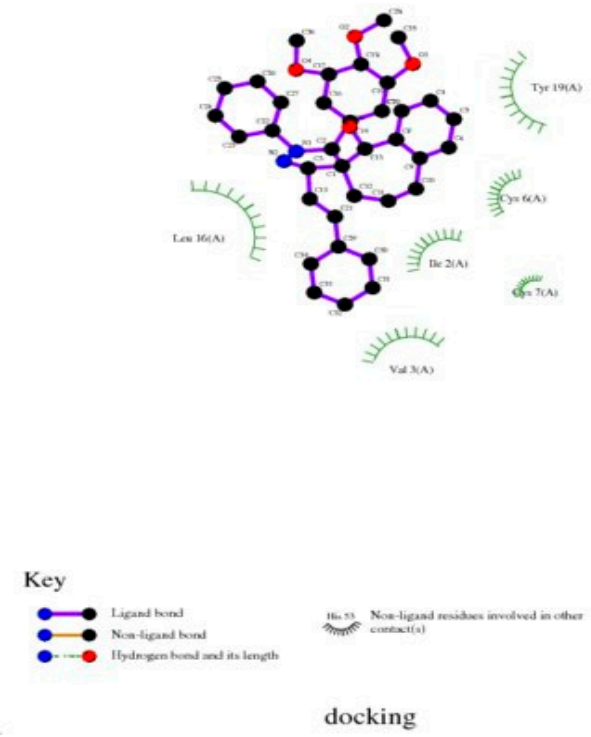

Compound (1)

Figure 7. *Cont.*

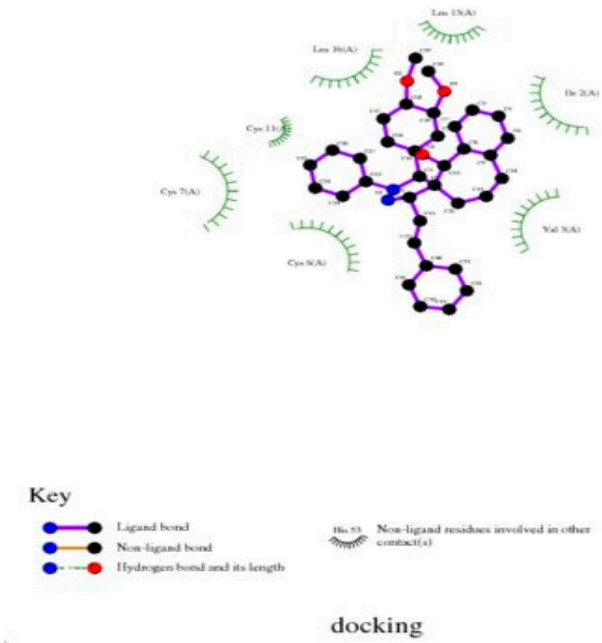

Compound (2)

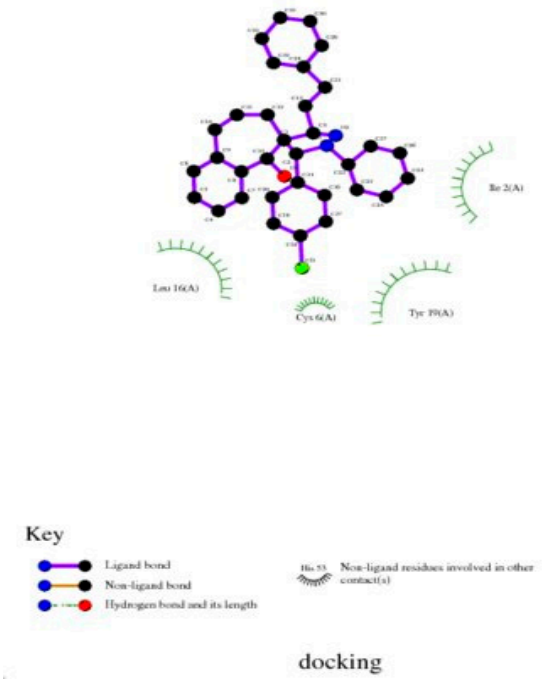

Compound (3)

Figure 7. 2D plot of interaction among spiropyrazoles products with 3tt8 receptor.

3.5. SEM Tests

The SEM test gotten from coins of Q235 steel existence and lack of 11×10^{-6} M spiropyrazoles products after dipping for three days obtain in Figure 8. The surfaces suffer from damaged corrosion attack in the blank. Due to the stress out when the composite appending in the solution, the morphology of the tests free surfaces was smoother. We observed a film creation which distributed in a random way on the whole surface of Q235 steel. This may be understood as being due to the spiropyrazole products adsorbed of the on Q235 steel which block the active center on alloy. This causes less contact among alloys and the aggressive enlivenments, and sequentially gives best protection effect [53,54].

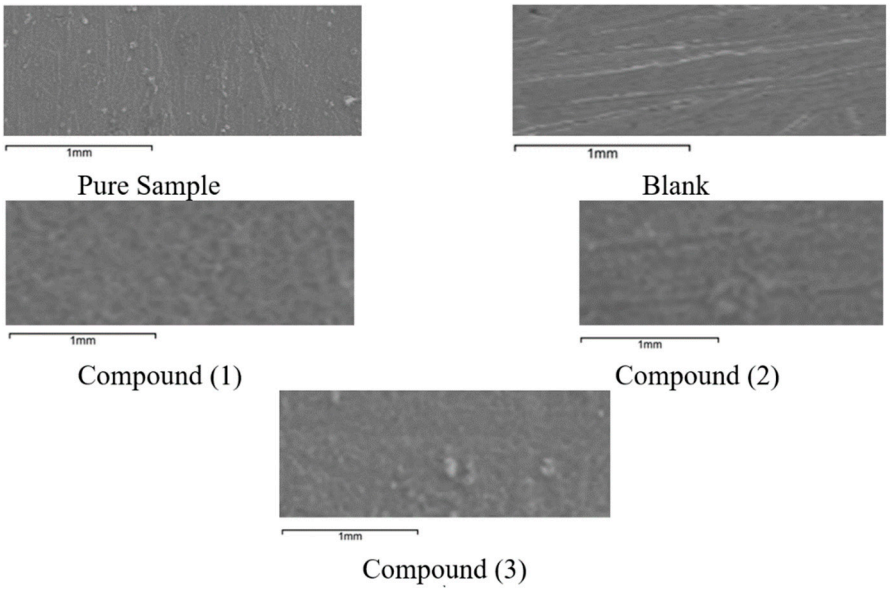

Figure 8. SEM images of Q235 steel in corrosive environments attendance and lack of unlike dose of 11×10^{-6} M spiropyrazoles.

3.6. EDS Test

The EDS tests were applied to measure the elements obtain on the surface of Q235 steel and after 3 days of coated in the lack and attendance of corrosive solution. Figure 9 gives the EDS data from the composition of Q235 steel only without the acid and presence spiropyrazoles. The EDS show that only oxygen and iron were detected, and the film passive was obtained with only Fe_2O_3.

The spectra give added lines, lead to the existence of C (C atoms of spiropyrazoles products). These data provide that the O and C atoms enclosed surface. The elemental detected is listed in Table 6.

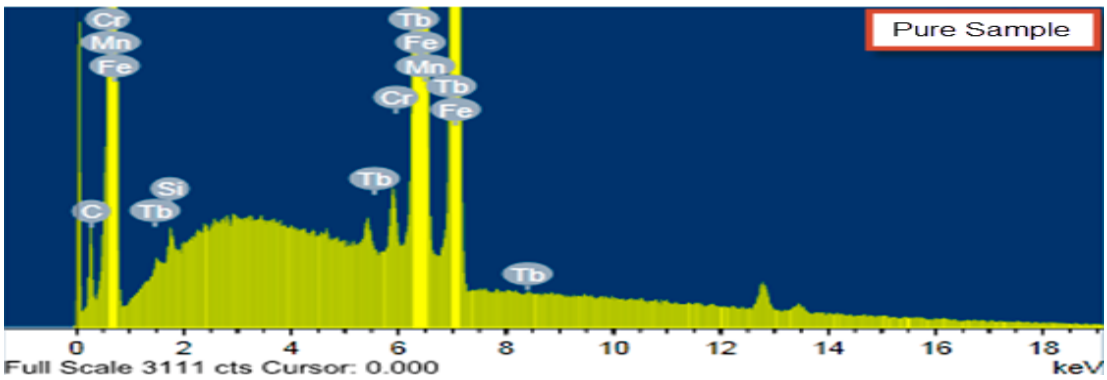

Figure 9. *Cont.*

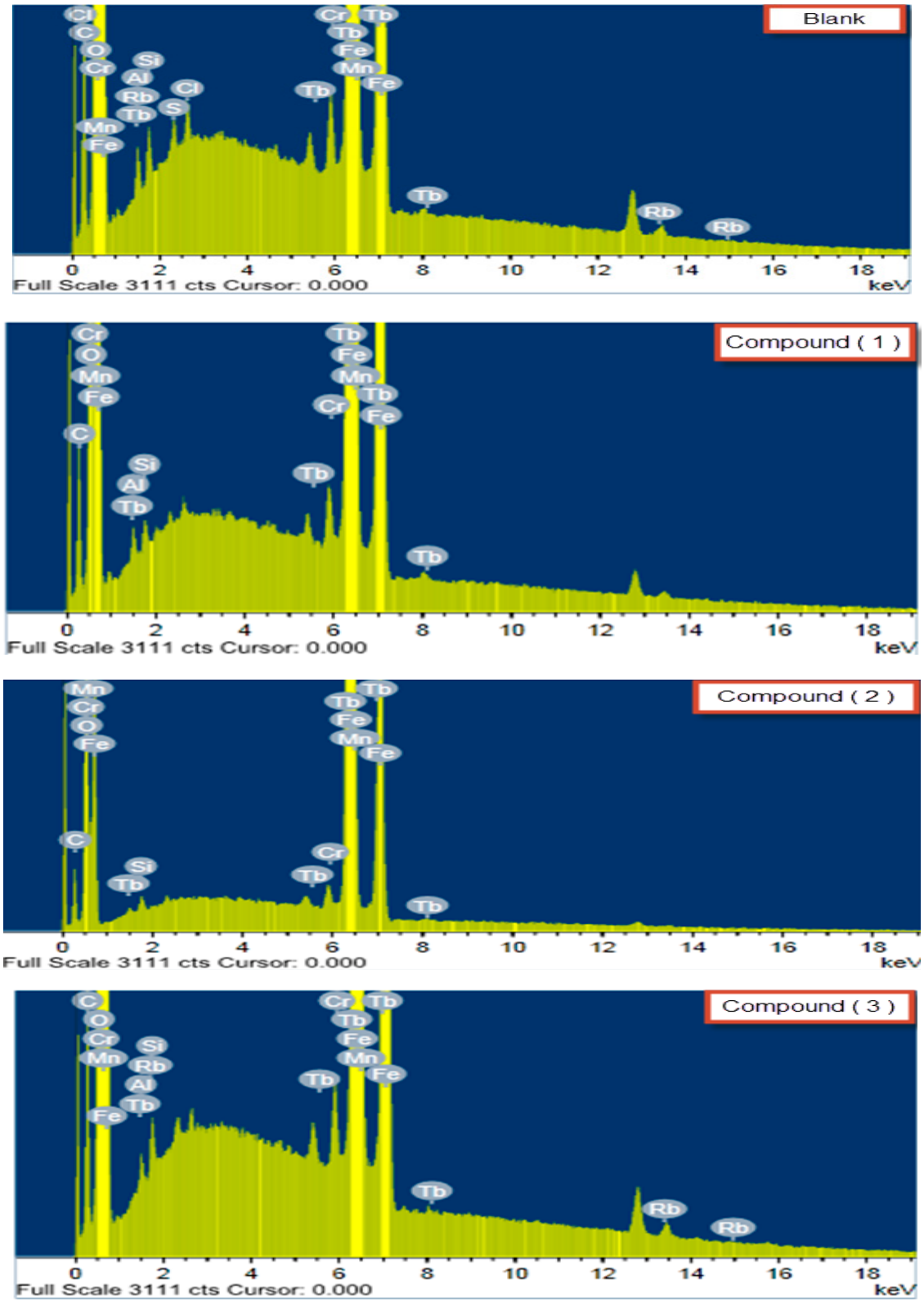

Figure 9. EDS study of Q235 steel after 3 days in corrosive environments attendance and lack of unlike dose of 11×10^{-6} M spiropyrazoles.

Table 6. Mass % of Q235 steel after 3 days in corrosive environments attendance and lack of unlike dose of 11×10^{-6} M spiropyrazoles.

(Mass %)	C	O	Al	Si	S	Cl	Cr	Mn	Fe	Rb	Tb
Pure Sample	7.08	–	0.28	0.27	–	–	0.24	0.46	87.14	–	4.53
Blank	11.98	17.64	0.29	0.30	0.14	0.18	0.19	0.39	65.54	0.46	2.89
Compound (1)	13.05	14.03	0.31	0.23	–	–	0.20	o.43	67.56	–	4.19
Compound (2)	12.68	16.99	0.01	0.26	–	–	0.19	0.41	65.70	–	3.76
Compound (3)	12.53	16.07	0.23	0.28	–	0.03	0.18	0.40	65.68	0.73	3.87

3.7. Quantum Chemical Calculations

The Mulliken charges and molecular orbital bends of spiropyrazole products given in Figure 10. Theoretical tests were obtained for only the forms of neutral, in order to gotten further insight into the experimental results. Data of quantum chemical chief to ΔE and E_{HOMO} and E_{LUMO} are measured and listed in Table 7. The improved or lesser negative E_{HOMO} is inhibitor related, the higher the trend of offering electrons to unoccupied d orbital of Q235 steel, and the progress of the corrosion hindrance. The lesser E_{LUMO}, the greater the acceptance of plain electrons from surface of Q235 steel [55,56]. ΔE assumed by the tests in case of spiropyrazole (1) is less than (3) (Table 7) given spiropyrazole (1) molecule will absorb more highest on alloy surface than others, due to electron easy transfer between HOMO and LUMO occurred among its adsorption on the surface of Q235 steel and the maximum of hindrance productivity [57]. It can be seen that all tests of quantum checking these results from experimental.

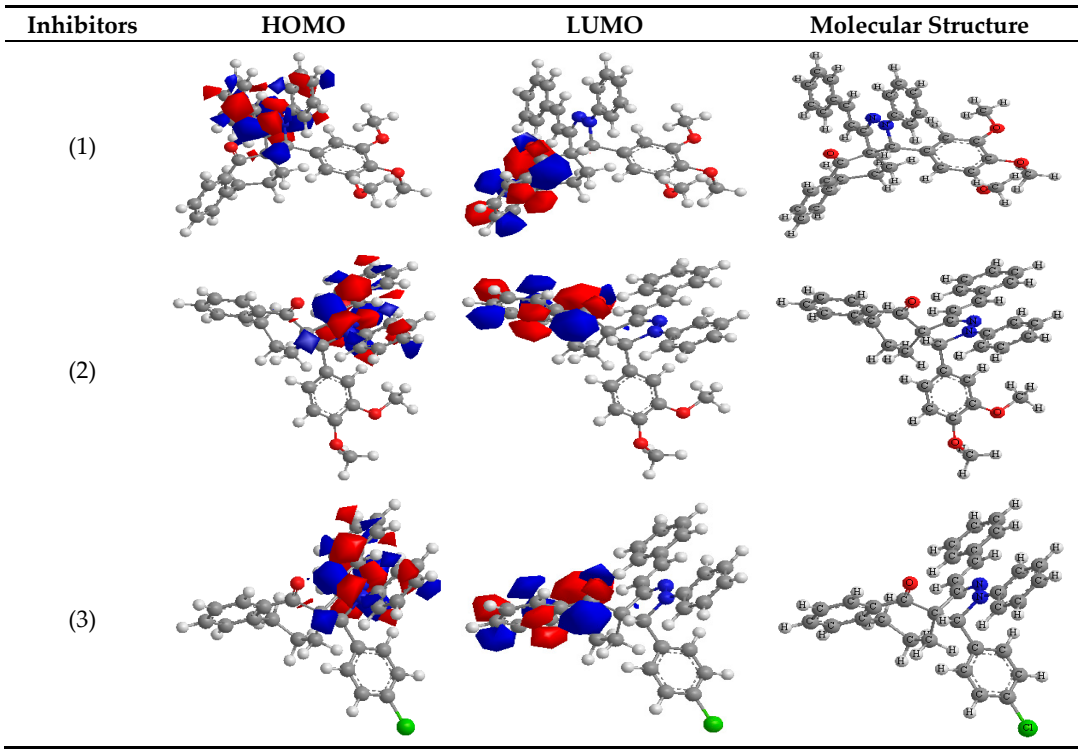

Figure 10. Molecular orbital bends of study spiropyrazoles.

Table 7. The measured quantum chemical propertiesfor spiropyrazoles products.

Quantum Chemical Properties	(1)	(2)	(3)
$-E_{HOMO}$ (eV)	8.006	8.007	8.021
$-E_{LUMO}$ (eV)	4.318	4.317	4.309
ΔE (eV)	3.688	3.690	3.712
η (eV)	1.844	1.845	1.856
σ $(eV)^{-1}$	0.542	0.542	6.165
−Pi (a.u)	6.162	6.162	0.538
χ (eV)	6.162	6.162	6.165
S $(eV)^{-1}$	0.271	0.271	0.269
ω (a.u)	3.081	3.081	3.0825
ΔN_{max}	3.341	3.339	3.321

3.8. Mechanism of Protection

From the results of electrochemical tests, the IE% relies on metal nature, dose, surface conditions, and the kind of spiropyrazole derivatives adsorption on Q235-steel.

The outcome data of corrosion data attendance of these inhibitors:

- With an increase in the dose of the inhibitor, the corrosion rate becomes lower
- The exchange in Tafel lines to extreme regions of potential.
- The %IE relies on excharge density and their equipment of adsorption centers in the molecule.

Metals such as iron, which are highly attractive to aromatic rings, were gotten to adsorb benzene rings in a flat direction. The order of breakdown of the %IE of the spiropyrazoles in the corrosion solution was in the following order: (1) > (2) > (3).

Spiropyrazoles (1) demonstrations best hindrance power because: (i) it has greater molecular size (558.25) that may enable best surface coated and bigger molecular area and (ii) its adsorption among 6 active sites (2-N and 4-O atoms). Spiropyrazoles (2) comes after (1) in %IE because it has fewer molecular size (528.24) and minus active site (1-O and 2-N atoms). Spiropyrazoles (3) is the smallest one in %IE, this is due to it having a minor molecular size (502.18), the appending of p-Cl group is electron withdrawing group with (σ Cl = +0.23), and its order of protection relies on the magnitude of their withdrawing character.

Concentration of the inhibitor is an important factor in adsorption. As illustrated in Figure 11, at the adsorption density less than monolayer (Figure 11a), most of the nucleus sites are still likely to be exposed to hydrochloric acid, as the inhibitor absorbs them less. When the adsorption intensity reaches monolayer adsorption (Figure 11b), some nucleus sites begin to cover with the barrier particles. At the maximum absorption density (Figure 11c), the inhibitor particles cover the entire surface, including the sites of the nucleus, and then complete inhibition occurs.

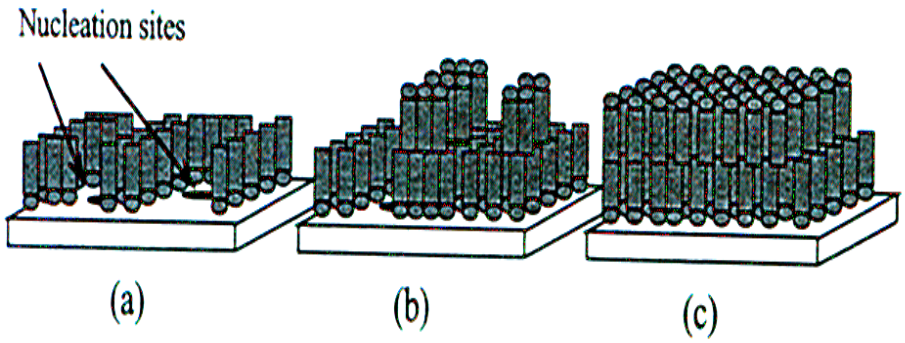

Figure 11. Adsorption diagrams for spiropyrazoles additives as inhibitors at: (**a**) Low concentration, (**b**) intermediate concentration, (**c**) high concentration on Q235 steel.

3.9. Conclusions

- All the spiropyrazole products are potentially brilliant corrosion inhibitors for Q235 steel. The structures of these spiropyrazole inhibtors as well as the presence of certain substituents play a vital role on their effectiveness anticorrosive agents.
- The results of EIS display enhancement in the charge transfer resistance and a decline in double layer capacitances. When adding an inhibitor and thus an increase in% IE due to an increase in the electrical double layer the thickness.
- The outcome values from electrochemical tests were in good agreement. The % IE of these spiropyrazoles is: (1)>(2)>(3).
- Molecular docking and binding energy calculations of spiropyrazolederivatives (1)–(3) with the receptor of 3tt8-hormone of crystal structure analysis of Cu human insulin derivative indicated that the spiropyrazoles are %IE of receptor of 3tt8-hormone.
- The morphology of protected and no protected Q235 steel was tested by SEM and EDX.
- Quantum calculation results demonstrated that the heteroatoms of N and O are the active sites ofthe spiropyrazole derivatives.

Author Contributions: Conceptualization, A.M.E. and H.M.H.; methodology, A.S., A.E.S.; software, A.M.E.; validation A.M.E.; A.S., A.E.S.; formal analysis, T.A.F.; investigation, A.E.S.; resources, T.A.F.; data curation, A.S.; writing—original draft preparation, H.M.H.; writing—review and editing, A.E.S.; visualization, A.M.E.; supervision, A.E.S.; project administration, T.A.F., A.M.E.; funding acquisition, A.M.E., H.M.H., A.S., A.E.S. and T.A.F. All authors have read and agreed to the published version of the manuscript.

Funding: This research received no external funding.

Conflicts of Interest: The authors declare no conflict of interest.

Data Availability Statement: The authors declare the data availability to share researchers to verify the results of an article, replicate the analysis, and conduct secondary analyses.

References

1. Hou, X.; Gao, L.; Cui, Z.; Yin, J. Corrosion and Protection of Metal in the Seawater Desalination. In *IOP Conference Series: Earth and Environmental Science*; IOP Publishing: Bristol, UK, 2018; Volume 108, p. 022037.
2. Świetlik, J.; Raczyk-Stanisławiak, U.; Piszora, P.; Nawrocki, J. Corrosion in drinking water pipes: The importance of green rusts. *Water Res.* **2012**, *46*, 1–10. [CrossRef]
3. Nawrocki, J.; Raczyk-Stanisławiak, U.; Świetlik, J.; Olejnik, A.; Sroka, M.J. Corrosion in a distribution system: Steady water and its composition. *Water Res.* **2010**, *44*, 1863–1872. [CrossRef]
4. Alamineh, E.A. Study of iron pipe corrosion in municipal water distribution system and its effect. *Am. J. Chem. Eng.* **2018**, *6*, 19–24. [CrossRef]
5. Revie, R.W. *Corrosion and Corrosion Control: An Introduction to Corrosion Science and Engineering*, 4th ed.; John Wiley & Sons: hoboken, NJ, USA, 2008.
6. Wahdan, M.; Hermas, A.; Morad, M. Corrosion inhibition of carbon-steels by propargyltriphenylphosphonium bromide in H_2SO_4 solution. *Mater. Chem. Phys.* **2002**, *76*, 111–118. [CrossRef]
7. Bentiss, F.; Lebrini, M.; Vezin, H.; Lagrenée, M. Experimental and theoretical study of 3-pyridyl-substituted 1, 2, 4-thiadiazole and 1, 3, 4-thiadiazole as corrosion inhibitors of mild steel in acidic media. *Mater. Chem. Phys.* **2004**, *87*, 18–23. [CrossRef]
8. Liu, X.; Okafor, P.; Zheng, Y. The inhibition of CO_2 corrosion of N80 mild steel in single liquid phase and liquid/particle two-phase flow by aminoethyl imidazoline derivatives. *Corros. Sci.* **2009**, *51*, 744–751. [CrossRef]
9. Al Maofari, A.; Ezznaydy, G.; Idouli, Y.; Guédira, F.; Zaydoun, S.; Labjar, N.; El, S. Inhibitive action of 3, 4′-bi-1, 2, 4-Triazole on the corrosion of copper in NaCl 3% solution. *J. Mater. Environ. Sci.* **2014**, *5*, 2081–2085.

10. Barouni, K.; Kassale, A.; Albourine, A.; Jbara, O.; Hammouti, B.; Bazzi, L. Amino acids as corrosion inhibitors for copper in nitric acid medium: Experimental and theoretical study. *J. Mater. Environ. Sci.* **2014**, *5*, 456–463.
11. Fouda, A.; Shalabi, K.; Elmogazy, H. Corrosion inhibition of α-brass in HNO3 by indole and 2-oxyindole. *J. Mater. Environ. Sci.* **2014**, *5*, 1691.
12. Ostovari, A.; Hoseinieh, S.; Peikari, M.; Shadizadeh, S.; Hashemi, S. Corrosion inhibition of mild steel in 1 M HCl solution by henna extract:A comparative study of the inhibition by henna and its constituents (Lawsone, Gallic acid, α-d-Glucose and Tannic acid). *Corros. Sci.* **2009**, *51*, 1935–1949. [CrossRef]
13. Bahrami, M.; Hosseini, S.; Pilvar, P. Experimental and theoretical investigation of organic compounds as inhibitors for mild steel corrosion in sulfuric acid medium. *Corros. Sci.* **2010**, *52*, 2793–2803. [CrossRef]
14. Solomon, M.; Umoren, S.; Udosoro, I.; Udoh, A. Inhibitive and adsorption behaviour of carboxymethyl cellulose on mild steel corrosion in sulphuric acid solution. *Corros. Sci.* **2010**, *52*, 1317–1325. [CrossRef]
15. Wang, H.-L.; Liu, R.-B.; Xin, J. Inhibiting effects of some mercapto-triazole derivatives on the corrosion of mild steel in 1.0 M HCl medium. *Corros. Sci.* **2004**, *46*, 2455–2466. [CrossRef]
16. Solmaz, R.; Kardas, G.; Yazici, B.; Erbil, M. Inhibition effect of rhodanine for corrosion of mild steel in hydrochloric acid solution. *Prot. Met.* **2005**, *41*, 581–585. [CrossRef]
17. Emregül, K.C.; Kurtaran, R.; Atakol, O. An investigation of chloride-substituted Schiff bases as corrosion inhibitors for steel. *Corros. Sci.* **2003**, *45*, 2803–2817. [CrossRef]
18. Chebabe, D.; Chikh, Z.A.; Hajjaji, N.; Srhiri, A.; Zucchi, F. Corrosion inhibition of Armco iron in 1 M HCl solution by alkyltriazoles. *Corros. Sci.* **2003**, *45*, 309–320. [CrossRef]
19. Liu, F.; Du, M.; Zhang, J.; Qiu, M. Electrochemical behavior of Q235 steel in saltwater saturated with carbon dioxide based on new imidazoline derivative inhibitor. *Corros. Sci.* **2009**, *51*, 102–109. [CrossRef]
20. Musa, A.Y.; Kadhum, A.A.H.; Mohamad, A.B.; Takriff, M.S. Experimental and theoretical study on the inhibition performance of triazole compounds for mild steel corrosion. *Corros. Sci.* **2010**, *52*, 3331–3340. [CrossRef]
21. Khaled, K.; Amin, M.A. Corrosion monitoring of mild steel in sulphuric acid solutions in presence of some thiazole derivatives–molecular dynamics, chemical and electrochemical studies. *Corros. Sci.* **2009**, *51*, 1964–1975. [CrossRef]
22. Quraishi, M.; Rafiquee, M.; Khan, S.; Saxena, N. Corrosion inhibition of aluminium in acid solutions by some imidazoline derivatives. *J. Appl. Electrochem.* **2007**, *37*, 1153–1162. [CrossRef]
23. Zhang, X.; Wang, F.; He, Y.; Du, Y. Study of the inhibition mechanism of imidazoline amide on CO_2 corrosion of Armco iron. *Corros. Sci.* **2001**, *43*, 1417–1431. [CrossRef]
24. Knag, M.; Bilkova, K.; Gulbrandsen, E.; Carlsen, P.; Sjöblom, J. Langmuir–Blodgett films of dococyltriethylammonium bromide and octadecanol on iron. Deposition and corrosion inhibitor performance in CO_2 containing brine. *Corros. Sci.* **2006**, *48*, 2592–2613. [CrossRef]
25. Wang, L.; Yin, G.-J.; Yin, J.-G. 2-Mercaptothiazoline and cetyl pyridinium chloride as inhibitors for the corrosion of a low carbon steel in phosphoric acid. *Corros. Sci.* **2001**, *43*, 1197–1202. [CrossRef]
26. Okafor, P.; Liu, X.; Zheng, Y. Corrosion inhibition of mild steel by ethylamino imidazoline derivative in CO_2-saturated solution. *Corros. Sci.* **2009**, *51*, 761–768. [CrossRef]
27. Zhang, J.; Liu, J.; Yu, W.; Yan, Y.; You, L.; Liu, L. Molecular modeling of the inhibition mechanism of 1-(2-aminoethyl)-2-alkyl-imidazoline. *Corros. Sci.* **2010**, *52*, 2059–2065. [CrossRef]
28. Eldesoky, A.; El-Bindary, M.; El-Sonbati, A.; Morgan, S.M. New eco-friendly corrosion inhibitors based on azo rhodanine derivatives for protection copper corrosion. *J. Mat. Environ. Sci.* **2015**, *6*, 2260–2276.
29. Eldesoky, A.; Diab, M.; El-Bindary, A.; El-Sonbati, A.; Seyam, H. Some antipyrine derivatives as corrosion inhibitors for copper in acidic medium: Experimental and quantum chemical molecular dynamics approach. *J. Mat. Environ. Sci.* **2015**, *6*, 2148–2165.
30. Bikadi, Z.; Hazai, E. Application of the PM6 semi-empirical method to modeling proteins enhances docking accuracy of AutoDock. *J. Cheminform.* **2009**, *1*, 15. [CrossRef]
31. Halgren, T.A. Merck molecular force field. I. Basis, form, scope, parameterization, and performance of MMFF94. *J. Comput. Chem.* **1996**, *17*, 490–519. [CrossRef]
32. Morris, G.M.; Goodsell, D.S.; Halliday, R.S.; Huey, R.; Hart, W.E.; Belew, R.K.; Olson, A.J. Automated docking using a lamarckian genetic algorithm and empirical binding free energy function. *J. Comp. Chem.* **1998**, *19*, 1639–1662. [CrossRef]

33. Riyadh, S.M.; Farghaly, T.A. Effect of solvent on the regioselective synthesis of spiropyrazoles. *Tetrahedron* **2012**, *68*, 9056–9060. [CrossRef]
34. Al-Khaldi, M.; Al-qahtani, K. Corrosion inhibition of steel by Coriander extracts in hydrochloric acid solution. *J. Mater. Environ. Sci.* **2013**, *4*, 593–600.
35. Schultze, J.; Wippermann, K. Inhibition of electrode processes on copper by AHT in acid solutions. *Electrochim. Acta* **1987**, *32*, 823–831. [CrossRef]
36. Silverman, D.; Carrico, J. Electrochemical impedance technique—A practical tool for corrosion prediction. *Corrosion* **1988**, *44*, 280–287. [CrossRef]
37. Macdonald, D.D.; McKubre, M.C. Impedance measurements in electrochemical systems. In *Modern Aspects of Electrochemistry*; Springer: Boston, MA, USA, 1982; pp. 61–150.
38. Mansfeld, F. Recording and analysis of AC impedance data for corrosion studies. *Corrosion* **1981**, *37*, 301–307. [CrossRef]
39. Gabrielli, C. *Identification of Electrochemical Processes by Frequency Response Analysis*; Technical Report No. 004; Solartron Instrumentation Group, Morris Bros. Ltd.: London, UK, 1980.
40. El Achouri, M.; Kertit, S.; Gouttaya, H.; Nciri, B.; Bensouda, Y.; Perez, L.; Infante, M.; Elkacemi, K. Corrosion inhibition of iron in 1 M HCl by some gemini surfactants in the series of alkanediyl-α, ω-bis-(dimethyl tetradecyl ammonium bromide). *Prog. Org. Coat.* **2001**, *43*, 267–273. [CrossRef]
41. Anejjar, A.; Zarrouk, A.; Salghi, R.; Zarrok, H.; Hmamou, D.B.; Hammouti, B.; Elmahi, B.; Al-Deyab, S. Studies on the inhibitive effect of the ammonium Iron (II) sulphate on the corrosion of carbon steel in HCl solution. *J. Mater. Environ. Sci.* **2013**, *4*, 583–592.
42. Mertens, S.; Xhoffer, C.; De Cooman, B.; Temmerman, E. Short-term deterioration of polymer-coated 55% Al-Zn—Part 1: Behavior of thin polymer films. *Corrosion* **1997**, *53*, 381–388. [CrossRef]
43. Trabanelli, G.; Monticelli, C.; Grassi, V.; Frignani, A. Electrochemical study on inhibitors of rebar corrosion in carbonated concrete. *Cem. Concr. Res.* **2005**, *35*, 1804–1813. [CrossRef]
44. Trowsdale, A.; Noble, B.; Harris, S.; Gibbins, I.; Thompson, G.; Wood, G. The influence of silicon carbide reinforcement on the pitting behaviour of aluminium. *Corros. Sci.* **1996**, *38*, 177–191. [CrossRef]
45. Reis, F.; De Melo, H.; Costa, I. EIS investigation on Al 5052 alloy surface preparation for self-assembling monolayer. *Electrochim. Acta* **2006**, *51*, 1780–1788. [CrossRef]
46. Lagrenee, M.; Mernari, B.; Bouanis, M.; Traisnel, M.; Bentiss, F. Study of the mechanism and inhibiting efficiency of 3, 5-bis (4-methylthiophenyl)-4H-1, 2, 4-triazole on mild steel corrosion in acidic media. *Corros. Sci.* **2002**, *44*, 573–588. [CrossRef]
47. McCafferty, E.; Hackerman, N. Kinetics of iron corrosion in concentrated acidic chloride solutions. *J. Electrochem. Soc.* **1972**, *119*, 999–1009. [CrossRef]
48. Ma, H.; Chen, S.; Niu, L.; Zhao, S.; Li, S.; Li, D. Inhibition of copper corrosion by several Schiff bases in aerated halide solutions. *J. Appl. Electrochem.* **2002**, *32*, 65–72. [CrossRef]
49. Kuş, E.; Mansfeld, F. An evaluation of the electrochemical frequency modulation (EFM) technique. *Corros. Sci.* **2006**, *48*, 965–979. [CrossRef]
50. Caignan, G.A.; Metcalf, S.K.; Holt, E.M. Thiophene substituted dihydropyridines. *J. Chem. Crystallogr.* **2000**, *30*, 415–422. [CrossRef]
51. Samie, F.; Tidblad, J.; Kucera, V.; Leygraf, C. Atmospheric corrosion effects of HNO_3—Method development and results on laboratory-exposed copper. *Atmos. Environ.* **2005**, *39*, 7362–7373. [CrossRef]
52. Refaat, H.M.; El-Badway, H.A.; Morgan, S.M. Molecular docking, geometrical structure, potentiometric and thermodynamic studies of moxifloxacin and its metal complexes. *J. Mol. Liq.* **2016**, *220*, 802–812. [CrossRef]
53. Prabhu, R.; Venkatesha, T.; Shanbhag, A.; Kulkarni, G.; Kalkhambkar, R. Inhibition effects of some Schiff's bases on the corrosion of mild steel in hydrochloric acid solution. *Corros. Sci.* **2008**, *50*, 3356–3362. [CrossRef]
54. Moretti, G.; Quartarone, G.; Tassan, A.; Zingales, A. Inhibition of mild steel corrosion in 1N sulphuric acid through indole. *Mater. Corros.* **1994**, *45*, 641–647. [CrossRef]
55. Samie, F.; Tidblad, J.; Kucera, V.; Leygraf, C. Atmospheric corrosion effects of HNO_3—Influence of concentration and air velocity on laboratory-exposed copper. *Atmos. Environ.* **2006**, *40*, 3631–3639. [CrossRef]

56. Lukovits, I.; Palfi, K.; Bako, I.; Kalman, E. LKP model of the inhibition mechanism of thiourea compounds. *Corrosion* **1997**, *53*, 915–919. [CrossRef]
57. Zhao, P.; Liang, Q.; Li, Y. Electrochemical, SEM/EDS and quantum chemical study of phthalocyanines as corrosion inhibitors for mild steel in 1 mol/l HCl. *Appl. Surf. Sci.* **2005**, *252*, 1596–1607. [CrossRef]